Copyright Notice

Institute of Communication Networks and Computer Engineering
University of Stuttgart
Pfaffenwaldring 47, D-70569 Stuttgart, Germany
Phone: ++49-711-685-8026, Fax: ++49-711-685-7983
email: mail@ikr.uni-stuttgart.de, http://www.ikr.uni-stuttgart.de

Generalized PSK for Improved Iterative Decoding and Demodulation of Coded DPSK Systems

Frieder Sanzi
Business Unit Logistics
Leuze Electronic GmbH + Co KG
In der Braike 1, D-73277 Owen/Teck, Germany
Email: friedrich.sanzi@leuze.de

Marc C. Necker
Institute of Communication Networks and Computer Engineering,
University of Stuttgart
Pfaffenwaldring 47, D-70569 Stuttgart, Germany
Email: necker@ikr.uni-stuttgart.de

***Abstract*— In this paper, the transmission of coded DPSK signals over a time-varying channel is considered. Coded DPSK is similar to a serially concatenated coding scheme where the inner encoder is replaced by a differential modulator. At the receiver side, the A Posteriori Probability (APP) calculation algorithmn is applied for differential demodulation, followed by an outer APP channel decoder. The Likelihood values at the output of the channel decoder are fed back to the differential demodulator in an iterative decoding loop. Such a system shows large coding gain for transmission over a time-varying flat fading channel if the receiver has perfect channel state information. However, perfect channel knowledge is normally not available at the receiver side. Therefore, joint channel estimation and demodulation has to be applied, leading to a dramatical performance degradation for conventional DPSK. In order to maintain the large coding gain even without any channel knowledge, we propose a novel concept for DPSK by applying regular and generalized PSK symbols in an alternating manner. We evaluate the proposed system on the basis of Extrinsic Information Transfer (EXIT) and Bit Error Ratio (BER) charts.**

I. Introduction

A differential modulator can be regarded as a recursive encoder of rate 1. Therefore, the differential demodulation of the signal can be realized by an APP decoder at the receiver side. In the following, we denote this process by APP demodulation. In the case of coded DPSK, the APP demodulator can be embedded in an iterative decoding loop together with the outer APP channel decoder. Using this iterative decoding loop, a low Bit Error Ratio (BER) can be achieved for transmission over a Gaussian channel. This becomes evident in the EXIT chart [1], since the characteristic curve of the APP demodulator reaches the point (1,1) for perfect a priori knowledge [2]. This property of the APP demodulator holds also for transmission over a flat fading channel under the assumption of perfect Channel State Information (CSI) at the receiver side.

Normally, CSI is not available and has to be estimated. Höher et al. [3] describe a method for joint channel estimation (CE) and demodulation using a super trellis at the receiver. This joint channel estimator and demodulator can also be embedded into the iterative loop in order to reduce the BER. However, its characteristic curve does not reach the point (1,1) in the EXIT chart. As a consequence, a tremendous loss in SNR occurs compared to the perfect CSI case.

In order to overcome the loss in SNR we propose a novel concept for differential modulation by alternating regular and generalized PSK symbols, where generalized PSK denotes PSK symbols with an arbitrary but regular angular difference in-between successive symbol points. This combination of regular and generalized PSK symbols was first proposed for totally blind channel estimation in [4], [5] and [6]. Using this concept, the characteristic curve of the joint channel estimator and demodulator reaches the point (1,1) in the EXIT chart. As a result, the performance of the joint channel estimator and demodulator comes close to the performance of the APP demodulator with perfect CSI.

This paper is structured as follows: In section II, we introduce the structure of the transmitter and the receiver. Subsequently, section III gives a detailled description of the joint channel estimator and demodulator applied in the receiver. Section IV discusses the system performance on the basis of EXIT charts and presents the results of the BER studies. Finally, section V concludes the paper.

II. System Model

A. Transmitter

The considered transmission system is depicted in Fig. 1, where the differential modulator is detailed in Fig. 2. The signal from the binary source is convolutionally encoded and interleaved. After interleaving, L successive bits $(c_{kL}, \ldots, c_{kL+L-1})$ are mapped onto one symbol d_k:

$$d_k = \sum_{n=0}^{L-1} c_{Lk+n} 2^n \quad , \quad d_k \in \{0, \ldots, M-1\}, \qquad (1)$$

where $M = 2^L$. In the remainder of the paper, we will only consider the case $L = 2$. However, our concepts also apply to other values of L. After the mapping stage, the intermediate

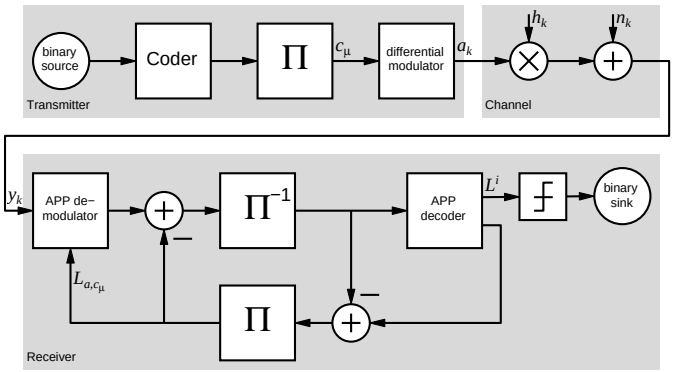

Fig. 1: System model

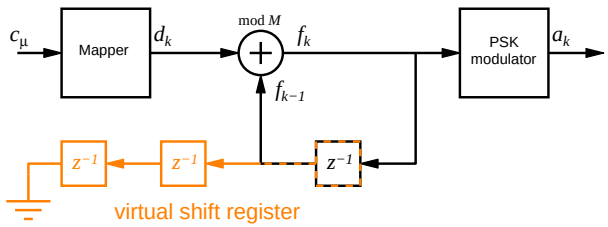

Fig. 2: Differential modulator, including virtual shift register

symbols $f_k = d_k \oplus f_{k-1}$ are calculated and mapped to the transmitted data symbols by the PSK modulator according to

$$a_k = \begin{cases} e^{j\frac{2\pi}{M}f_k} & \text{for } k \text{ even} \\ e^{j\frac{2\pi}{\eta}f_k} & \text{for } k \text{ odd} \end{cases} . \tag{2}$$

That is, every other symbol is a regular PSK symbol. All remaining symbols are generalized PSK symbols as shown in Fig. 3 with signal points $\mathcal{S}_i^4$:

$$\mathcal{S}_i^4 = e^{ji\frac{2\pi}{\eta}} \quad , 0 \le i \le 3,\ \eta \in \mathbb{R} \ . \tag{3}$$

In the coder, we use a recursive systematic convolutional code with feedback polynomial $G_\mathrm{r} = 7_8$, feed-forward polynomial $G = 5_8$, memory 2 and code rate $R_\mathrm{c} = 0.5$. The rather small memory size of 2 is motivated by the results presented in [7], where it was found that smaller memory sizes deliver better BER performance. Note that in the following all E_b/N_0-values are given with respect to the overall information rate $R = R_\mathrm{c}$.

B. Channel Model

The transmitted signal a_k is attenuated by the channel's fading coefficient h_k and corrupted by complex AWGN n_k with component-wise variance $\sigma_n^2 = N_0/2$. The fading coefficient was simulated following the model introduced in [8]:

$$h_k = \lim_{Z\to\infty} \frac{1}{\sqrt{Z}} \sum_{m=1}^{Z} e^{j\theta_m} e^{j2\pi f_{\mathrm{D}_m} k T_s} \quad , \tag{4}$$

where $f_{\mathrm{D}_m} \le f_{\mathrm{D,max}}$ is the Doppler shift and T_s is the symbol duration. For each of the Z paths, the phase-shift θ_m and the Doppler-shift f_{D_m} are randomly chosen from the corresponding probability density function (pdf) $p_\theta(\theta)$ or $p_{f_\mathrm{D}}(f_\mathrm{D})$ of the channel model. For the simulations, the number of paths was set to $Z = 200$.

For the channel model in our simulations, the phase θ is uniformly distributed between 0 and 2π. The pdf of the Doppler frequency is assumed to be of Jakes' type

$$p_{f_\mathrm{D}}(f_\mathrm{D}) = \begin{cases} \frac{1}{\pi f_{\mathrm{D,max}}\sqrt{1-(f_\mathrm{D}/f_{\mathrm{D,max}})^2}} & |f_\mathrm{D}| \le f_{\mathrm{D,max}} \\ 0 & \text{otherwise} \end{cases} , \tag{5}$$

whereby $f_{\mathrm{D,max}}$ is the maximal Doppler shift.

With these assumptions the auto-correlation function $R_{\Delta k} = \mathrm{E}\{h_{k+\Delta k} \cdot h_k^*\}$ of h_k is given by

$$R_{\Delta k} = J_0(2\pi f_{\mathrm{D,max}} \cdot \Delta k \cdot T_s) \ . \tag{6}$$

J_0 is the Bessel function of zero order, and * denotes the conjugate complex operation. Please refer to [8] for the derivation of (6).

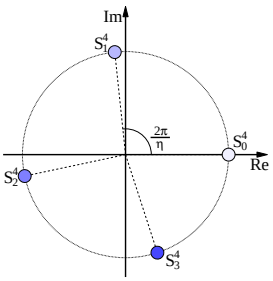

Fig. 3: Generalized 4-PSK

C. Receiver

At the receiver, the received signal $y_k = h_k a_k + n_k$ is demodulated within the APP demodulator, which performs a joint channel estimation and demodulation as described in [3] by building up a super-trellis using the virtual shift register indicated in Fig. 2. The APP demodulator is embedded in an iterative decoding loop with a standard APP decoder. After several iterations, the L-values [9] on the information bits are hard-decided and fed to the binary sink.

III. Joint Channel Estimator and Demodulator

For the joint channel estimator and demodulator, the symbol-by-symbol MAP-algorithm is applied to an appropriately chosen metric. To help understanding, the symbols f_k at the transmitter in Fig. 2 can be thought of being put into a virtual shift register at the output of the feedback delay element, as sketched in Fig. 2. Due to this "artificial grouping", the corresponding super-trellis exploits the time continuity of the flat fading channel at the receiver.

The metric increment γ_k in the super-trellis is given by

$$\gamma_k = -\frac{|y_k - \hat{h}_k \cdot \hat{a}_k|^2}{2 \cdot \sigma_t^2} + \sum_{i=0}^{L-1} \hat{q}_{Lk+i} \cdot L_{\mathrm{a},c_{Lk+i}} \tag{7}$$

with estimated channel coefficient

$$\hat{h}_k = \sum_{i=1}^{m} u_i \cdot \frac{y_{k-i}}{\hat{a}_{k-i}} \ . \tag{8}$$

The $\hat{a}_k$ denote the hypothesized transmitted data symbol according to the trellis structure. The $L_{\mathrm{a},c_{Lk+i}}$ in (7) are the *a-priori* L-values of the coded bits c_μ which are fed to the joint channel estimator and demodulator. The bits $\hat{q}_{Lk+i}$ in the sum in (7) result from the hard demapping of the hypothesized symbol $\hat{d}_k$ according to the trellis structure. m is the prediction order. In the following paragraphs, we will describe the calculation of the prediction coefficients u_i in (8) and the derivation of the variance $2 \cdot \sigma_t^2$ of the error in (7).

For the calculation of the linear prediction coefficients, we assume that the current state in the trellis is the actual correct state. Then, $\frac{y_{k-i}}{\hat{a}_{k-i}} = \hat{h}_{k-i}$, and (8) can be expressed as (cmp. method OLPC in [10])

$$\hat{h}_k = \sum_{i=1}^{m} u_i \cdot \hat{h}_{k-i} \ , \tag{9}$$

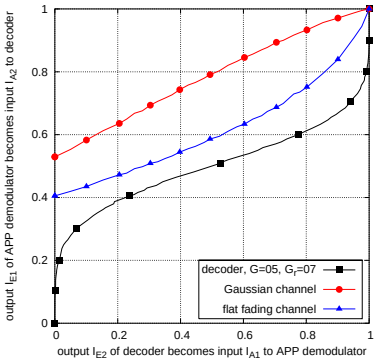

Fig. 4: EXIT chart for systems with Gauss channel and flat fading channel with perfect CSI, $f_{\mathrm{D,max}}T_s = 0.01$ and $E_b/N_0 = 4\mathrm{dB}$

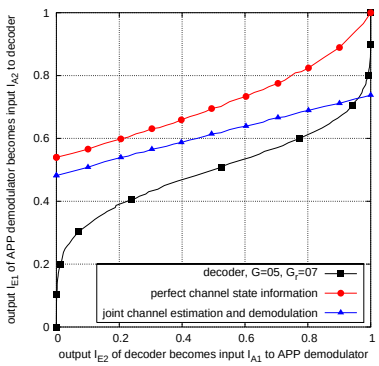

Fig. 5: EXIT chart for systems with flat fading channel with perfect CSI and with joint CE and demodulation, $f_{\mathrm{D,max}}T_s = 0.01$ and $E_b/N_0 = 6\mathrm{dB}$

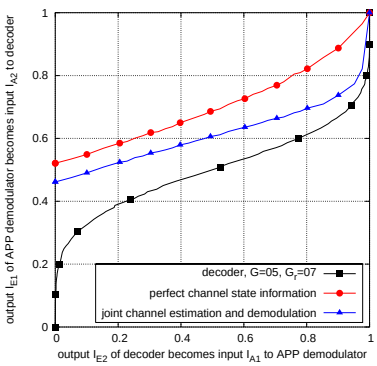

Fig. 6: Flat fading channel with perfect CSI and with joint CE and demodulation with alternating PSK schemes, $\eta = 3.6$, $f_{\mathrm{D,max}}T_s = 0.01$ and $E_b/N_0 = 6\mathrm{dB}$

whereby

$$\hat{h}_{k-i} = h_{k-i} + \frac{n_{k-i}}{\hat{a}_{k-i}} \ . \tag{10}$$

Taking (6) and (10) into account, and assuming that a_k and n_k are not correlated, we can compute the expected value

$$\mathrm{E}\left\{\hat{h}_{k-i} \cdot \hat{h}^*_{k-\tilde{i}}\right\} = R_{\tilde{i}-i} + \delta_{\tilde{i}-i} \cdot \frac{N_0}{|\hat{a}_{k-i}|^2} = R_{\tilde{i}-i} + \delta_{\tilde{i}-i} \cdot \frac{N_0}{\beta} \ , \tag{11}$$

where $\beta = |\hat{a}_{k-i}|^2$ is constant, since we consider a PSK modulation scheme. Finally, we can calculate the expected value

$$\mathrm{E}\left\{h_k \cdot \hat{h}^*_{k-i}\right\} = R_i \ . \tag{12}$$

We calculate the linear prediction coefficients solving the Wiener-Hopf equation in order to minimize the mean squared error $\mathrm{E}\left\{\left|h_k - \hat{h}_k\right|^2\right\}$. Therefore, the linear prediction coefficients are:

$$(u_1, \ldots, u_m) = \mathbf{r}^T \cdot \mathbf{R}^{-1} \tag{13}$$

Taking (12) into account, the vector $\mathbf{r}^T$ can be calculated as:

$$\mathbf{r}^T = (R_1, \ldots, R_m) \ . \tag{14}$$

Using (11), we obtain the matrix $\mathbf{R}$ as:

$$\mathbf{R} = \begin{pmatrix} 1 + \frac{N_0}{\beta} & R_1 & \cdots & R_{m-1} \\ R_{-1} & 1 + \frac{N_0}{\beta} & & R_{m-2} \\ \vdots & & \ddots & \vdots \\ R_{-m+1} & \cdots & R_{-1} & 1 + \frac{N_0}{\beta} \end{pmatrix} \ . \tag{15}$$

The minimum mean squared error results to:

$$J_{\min} = 1 - \mathbf{r}^T \cdot \mathbf{R}^{-1} \cdot \mathbf{r}^* \ . \tag{16}$$

Therefore, the term $2 \cdot \sigma_t^2$ in (7) yields to:

$$2 \cdot \sigma_t^2 = N_0 + J_{\min} \cdot \beta \ . \tag{17}$$

In the method OLPC in [10], each state in the trellis has its own linear prediction coefficients and minimum mean squared error. In contrast, due to the fact that in our case $\beta = |\hat{a}_{k-i}|^2$ is constant, all states in the trellis have the same linear prediction coefficients and minimum mean squared error.

IV. Results

A. EXIT chart analysis

Figure 4 shows the EXIT chart for a conventional system using a regular DPSK modulation scheme. Two characteristic curves of the APP demodulator are depicted; one for the Gaussian channel and the other for a flat fading channel using perfect CSI with $f_{\mathrm{D,max}}T_s = 0.01$ at $E_b/N_0 = 4\mathrm{dB}$. As reported in [2], the curve of the Gaussian channel reaches the point (1,1) in the EXIT chart. As a consequence of this property, a low bit error ratio can be achieved using the iterative decoding loop. As can be seen in Fig. 4, this property holds also for the charateristic curve of the flat fading channel under the assumption of perfect CSI at the receiver.

In Fig. 5, the EXIT chart for a flat fading channel with $f_{\mathrm{D,max}}T_s = 0.01$ at $E_b/N_0 = 6\mathrm{dB}$ is depicted. Two curves of the APP demodulator are given; one with perfect CSI and the other with the joint channel estimation and demodulation described in section III. While the curve for perfect CSI reaches the point (1,1), this property holds not any more for the joint channel estimator and demodulator. Its endpoint drops down to the point (1,0.714) for perfect a-priori knowledge I_{A1}. Due to this property, the curve looks similar to the curve of a demapper in a bit-interleaved coded modulation scheme [11]. Therefore, the system with the joint channel estimator and demodulator exhibits a bit error floor.

In order to bend up the tail of the charateristic curve of the joint channel estimator and demodulator to the point (1,1), we propose a system which transmits regular and general PSK in an alternating manner, as it was described in section II-A. The EXIT chart of the proposed system is shown in Fig. 6 with $\eta = 3.6$. Now, using this novel concept for DPSK, both curves reach the point (1,1) in the EXIT chart. Therefore, the error floor of the conventional system is removed.

In Fig. 7 the characteristic curves of the joint channel estimator and demodulator for the regular and the alternating DPSK scheme are depicted in order to clearly show the difference. Since the proposed alternating DPSK scheme reaches the point (1,1) in the EXIT chart, the error floor of the conventional system is eliminated resulting in a dramatical increase of the performance of the overall system. This per-

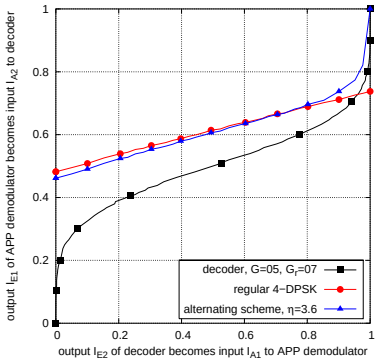

Fig. 7: Flat fading channel with joint CE and demodulation for conventional and proposed system, $\eta = 3.6$, $f_{\mathrm{D,max}}T_s = 0.01$ and $E_b/N_0 = 6\mathrm{dB}$

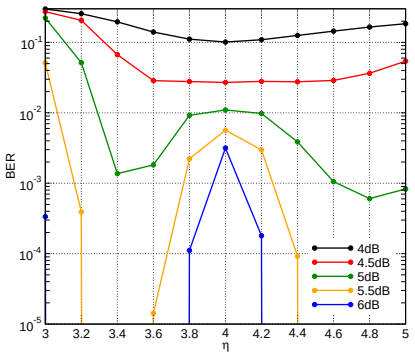

Fig. 8: BER over η for different values of E_b/N_0, $f_{\mathrm{D,max}}T_s = 0.01$, 19 iterations

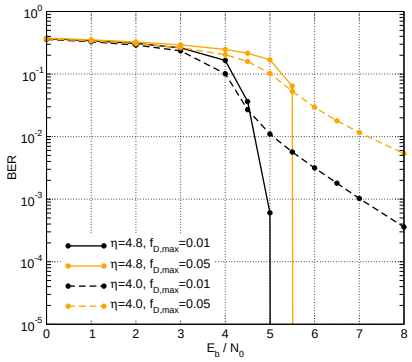

Fig. 9: BER charts for different values of η and $f_{\mathrm{D,max}}T_s$, 19 iterations

formance improvement is achieved without adding additional redundancy while keeping the complexity constant.

B. BER results

For the simulations, the block length of the differential modulator is set to 10000 symbols. The interleaving is done over 5 blocks resulting in an interleaver size of 100000 bits. The order m of the linear predictor is set to 2, which is a good trade-off between complexity and performance [10]. The number of iterations in the iterative decoding loop was set to 19, and a total of 10,000,000 information bits was transmitted during one simulation run.

The characteristics of the EXIT charts reflect themselves in the BER chart of Fig. 8, which plots the BER over the parameter η for different E_b/N_0. A conventional system which applies regular PSK corresponds to the choice $\eta = 4$. From Fig. 8 we can see that for $\eta = 4$ the BER reaches a local maximum for relevant values of E_b/N_0. From the EXIT chart we know that for $\eta = 4$ the characteristic curve of the APP demodulator ends at $I_{\mathrm{E1}} = 0.714$, while this ending point moves up to $I_{\mathrm{E1}} = 1$ as η is increased or decreased. Consequently, the BER performance greatly improves as η is increased or decreased. The maximum is achieved for η between 3.4 and 3.6 and η around 4.8. If η is increased or decreased further, the performance becomes worse again. Especially for $\eta = 3$ the BER performance is extremely poor, as the resulting 3-PSK modulation scheme occupies one signal point twice.

In order to study the impact of the maximum Doppler shift, Fig. 9 plots the BER over the E_b/N_0 for the normalized maximum Doppler shifts $f_{\mathrm{D,max}}T_s = 0.01$ and $f_{\mathrm{D,max}}T_s = 0.05$. Plotted are the BER curves for the conventional PSK system with $\eta = 4$ and for the system applying the modulation scheme with $\eta = 4.8$, which was found to deliver the best performance in the previous paragraph. At low E_b/N_0, the performance of the conventional PSK scheme first drops below the performance with $\eta = 4.8$. However, with $\eta = 4.8$, we quickly outperform the conventional system as E_b/N_0 increases. The performance improvement is quite significant, as we can observe steep turbo cliffs for $\eta = 4.8$ in Fig. 9.

V. Conclusion

We showed how the performance of a coded DPSK system can dramatically be improved by using alternating regular and generalized PSK symbols. Up to now, a realistic receiver, which does not have access to perfect channel knowledge, suffered from a significant performance loss compared to idealistic receivers which have perfect channel state information. However, with the combination of modulation schemes as presented in this paper, a receiver which does not have any *a-priori* channel knowledge can achieve almost the same BER performance as a receiver which has perfect channel knowledge. Eventually, this new scheme makes the application of differential modulation schemes very attractive, as we can now easily outperform systems with coherent modulation even if perfect channel state information is not available at the receiver.

References

[1] S. ten Brink, "Convergence behavior of iteratively decoded parallel concatenated codes," *IEEE Trans. on Comm.*, vol. 49, no. 10, 2001.

[2] J. Hagenauer, "The Exit Chart," in *Proc. 12th European Signal Processing Conference (EUSIPCO 2004)*, Vienna, Austria, September 2004.

[3] P. Höher and J. Lodge, "Turbo DPSK: Iterative differential PSK demodulation and channel decoding," *IEEE Trans. Commun.*, vol. 47, no. 6, 1999.

[4] M. C. Necker and G. L. Stüber, "Totally blind channel estimation for OFDM over fast varying mobile channels," in *Proc. IEEE Intern. Conf. on Comm.*, 2002.

[5] ——, "Totally blind channel estimation for OFDM on fast varying mobile radio channels," *IEEE Trans. on Wireless Communications*, vol. 3, no. 5, 2004.

[6] M. C. Necker and F. Sanzi, "Generalized 8-PSK for totally blind channel estimation in OFDM," in *Proc. IEEE VTC 2004 Spring*, Milano, Italy, May 2004.

[7] I. D. Marsland and P. T. Mathiopoulos, "On the performance of iterative noncoherent detection of coded M-PSK signals," *IEEE Transactions on Communications*, vol. 48, no. 4, April 2000.

[8] P. Höher, "A statistical discrete-time model for the WSSUS multipath channel," *IEEE Trans. on Veh. Tech.*, vol. 41, no. 4, 1992.

[9] J. Hagenauer, E. Offer, and L. Papke, "Iterative decoding of binary block and convolutional codes," *IEEE Trans. on Inform. Theory.*, vol. 42, no. 2, 1996.

[10] M. C. Necker and F. Sanzi, "Impact of linear prediction coefficients on totally blind app channel estimation," in *Proc. ITG SCC*, Erlangen, Germany, January 2004.

[11] S. Pfletschinger and F. Sanzi, "Iterative demapping for OFDM with zero-padding or cyclic prefix," in *Proc. IEEE ICC 2004*, Paris, France, June 2004.